SHOT PEENING VERSUS LASER SHOCK PROCESSING

Grzegorz Banaś and Frederick V. Lawrence, Jr.,
University of Illinois at Urbana-Champaign, 205 N. Mathews Ave.,
Urbana, Illinois 61801, U.S.A.

ABSTRACT

Shot peening and laser shock processing effect on residual stress, hardness, and fatigue behaviour of welded 18 Ni (250) maraging steel is presented in this paper. Initiation-propagation model was used for fatigue strength predictions of as-welded, shot-peened, and laser-shock-treated specimens. Elastic stress concentration factor (K_t) was determined using finite element analysis considering both tensile and bending stresses. Laser shock processing as well as shot peening altered both hardness and residual stress state of welded specimens; there was an increase in both hardness and compressive residual stresses. Fatigue strength was also higher, however, laser shock processing gave better performance in longer lives ($>10^5$ cycles), while in shorter lives ($\leq 10^5$ cycles) no significant difference was found between shot peening and laser shock processing. The comparison of predicted and experimental results showed an agreement within 10 -20 %.

KEYWORDS

Weldments, shot peening, laser shock precessing, metallic fatigue, residual stresses, hardness.

INTRODUCTION

Shot peening, flyer-plate technique, explosive treatment, and cold rolling are the methods of strain hardening which have been used for many years in the industrial applications. Each of these techniques requires to use a specialized installation and instrumentation which may vary for different specific components. For instance the requirement of explosives or high velocity driver plates or projectiles makes the practical use of those methods difficult. Shot peening is the most common technique which could be difficult to use when an access to treated surface is limited, while cold rolling can be used only for geometrically regular parts.

Many fundamental investigations have been conducted to determine the laser-material interaction [1 - 6]. The effects of high power laser radiation on absorbing surfaces and the potential of their application in materials processing have been particularly studied [7 - 10] using both continuous and pulsed lasers. Figure 1 shows the operational regimes for various laser-processing techniques. Laser shock processing (LSP) uses the radiation emitted by a high-power pulse laser to generate a short duration (<1 ms) high amplitude pressure pulse (>10^9 W/cm^2 in power density) at the surface of the material.

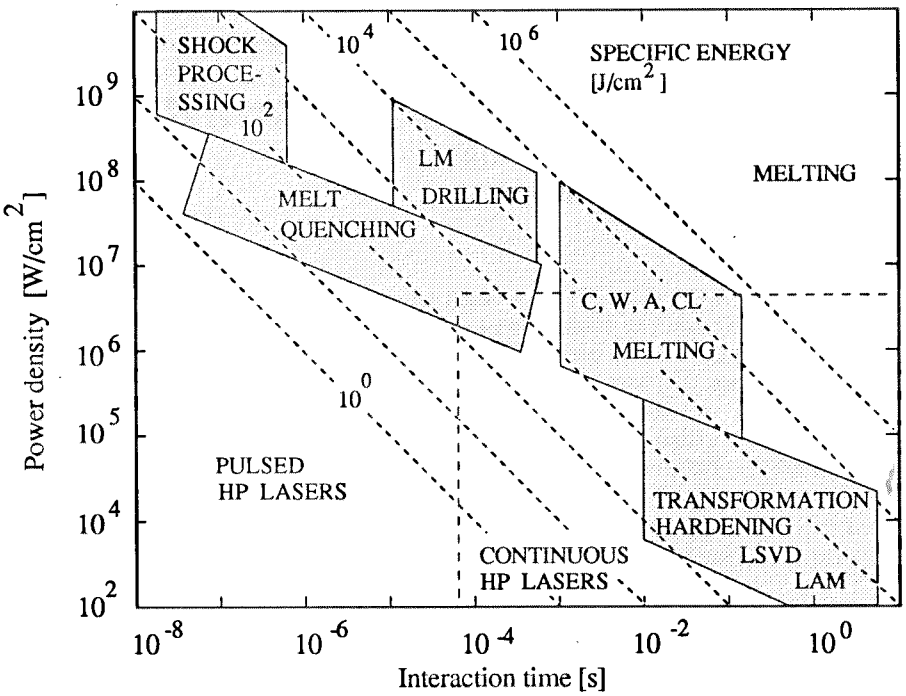

Fig. 1 Operational regimes for various laser processing techniques: C - cutting, W - welding, A - alloying, CL - cladding, LM - laser machining, LAM - laser aided manufacturing, LSVD - laser chemical vapor deposition [7].

Generation of the high-amplitude stress waves requires covering the surface to be shocked with a thin layer of a sacrificial material with a low heat of vaporization (e.g. black paint or lead) to enhance absorption of the laser radiation and to protect the surface of the specimen from melting and vaporization (Fig. 2). A material which is transparent to laser light is placed on top of the first layer. The surface of the sacrificial material is vaporized when it is struck by laser radiation. The vaporized gas is trapped between the specimen surface and the transparent overlay. During further expansion

by absorbing radiation from the laser beam, the pressure increases to extremely high levels causing a pressure pulse to react against the specimen surface and to travel through the metal as a wave. The transparent overlay acts to confine the vapor and enhance the amplitude and duration of the pressure pulse acting on the surface; see Fig. 2. The peak pressures generated at the surface of the specimen are a function of the incident laser power density and the properties of the transparent overlay.

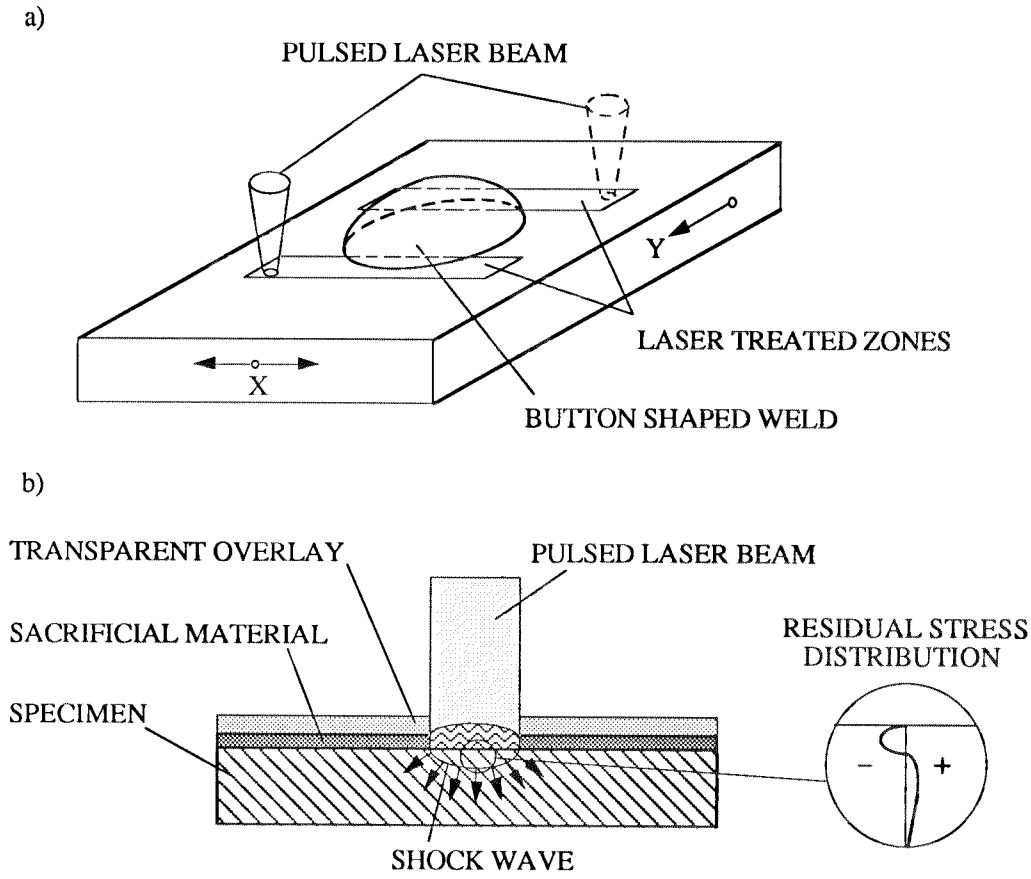

Fig. 2 Laser shock processing; a) experimental setup, b) scheme of the vaporization and pressure reactions at the specimen surface during laser irradiation.

EXPERIMENTAL PROCEDURES

Material and specimen fabrication

18 Ni (250) maraging steel was used in this study which had the composition and mechanical properties after aging given in Tables 1 and 2.

The 18 Ni (250) maraging steel was derived as a plate with the thickness of 4.15 mm which was saw-cut into smaller plates that included ten test-pieces. Two kinds of specimens were fabricated:
- button-shaped bead-on-plate -- by depositing a button-like weld bead on one side of the plate using a semi-automatic GMA welding apparatus; for laser shock processing.
- double bead-on-plate -- by depositing a weld bead on both sides of the plate using a semi-automatic GMA welding apparatus; for shot peening

Table 1 Chemical composition of 18 Ni (250) maraging steel.[a, b]

C%	Mn%	P%	S%	Si%	Ni%	Cr%	Mo%	Cu%	Ti%	Co%	Al%
0.02	0.01	0.008	0.007	0.08	18.29	0.03	5.40	0.04	0.34	7.31	0.01

[a] Chemical composition analysis was done by CHICAGO SPECTRO SERVICE LABORATORY, Inc.
[b] Iron -- balance.

Table 2 Mechanical properties of 18 Ni (250) maraging steel after aging 5 hrs at 480 °C.[a]

Monotonic properties		
Elastic modulus, GPa	E	186
Hardness, HRC		50-52
Yield strength (0.2%), MPa	S_y	1,700
Ultimate tensile strength, MPa	S_u	1,600
Reduction in area	%RA	55
True fracture strength, MPa	σ_f	2,146
True fracture ductility	ε_f	0.80
Strength coefficient, MPa	K	2,160
Strain hardening exponent	n	0.03
Cyclic properties		
Fatigue ductility coefficient	ε'_f	0.80
Fatigue ductility exponent	c	-0.61
Fatigue strength coefficient, MPa	σ'_f	2,232
Fatigue strength exponent	b	-0.063
Cyclic strength coefficient, MPa	K'	2,282
Cyclic strain hardening exponent	n'	0.10
Cyclic yield strength, MPa	S'_y	1,245
Transition fatigue life, reversals	$2N_t$	330
Propagation properties		
Fracture toughness, MPa$\sqrt{m}$ (R = 0)	K_C	330

[a] All mechanical properties were obtained from experiments [11] and calculations [12].

Test pieces were saw-cut into strips, machined to dimensions shown on Figs, 3 a and b, and heat-treated (aging at 480 °C for 5 hours in air).

Post-weld treatments

Laser shock processing. The specimens (Fig. 3a) were coated with a thin layer (0.1 mm) of black paint and were placed under a 3.5 mm of water during laser irradiation. The thin layer of black paint provided a sacrificial material with a low heat of vaporization that enhanced laser coupling and, to some degree, protected the surface of the specimen from melting and vaporization. The water overlay acted to confine the vaporized sacrificial material and was previously found to be effective in increasing the amplitude of the shock wave [13].

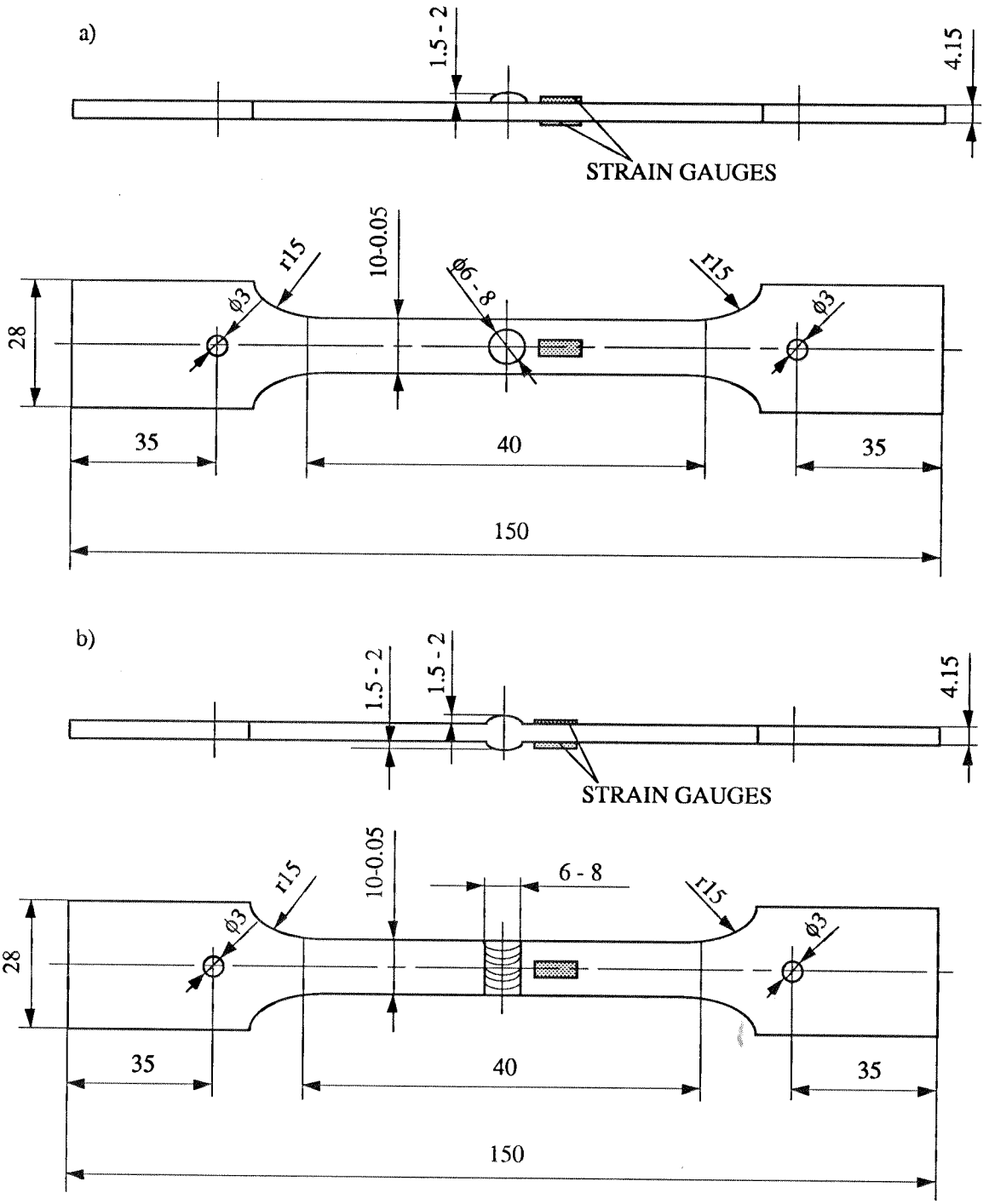

Fig. 3 Fatigue test specimens; a) with button-shaped beat-on-plate for laser shock precessing, b) with double beat-on-plate for shot peening.

Experiments were performed using a laser consisting of a 100 MHz Nd:YAG (λ = 1.06 μm) oscillator followed by a Pockels cell for pulse selection. The oscillator pulse was injected into a regenerative amplifier capable of providing 0.5 mJ pulses with 100 ps pulse width and up to 1 kHz repetition rate. These pulses were cleaned using a switch-out Pockels cell. A double-pass amplifier operating at 8 Hz repetition rate was used to amplify the laser pulses to the 30 mJ level. The specimens were irradiated with 20 mJ pulses (100 ps pulse width) at 8 Hz repetition rate. Since the laser beam was focussed to 0.1 mm spot diameter at the specimen, a technique of pulse overlapping was used in order to completely cover the weldment zone (~28 mm^2); see Fig. 2. A computer controlled X-Y table was used to move the water tank containing the specimen in the required directions while processing.

Shot peening. Specially designed apparatus was used for shot peening. The specimens (Fig. 3b) were peened using 0.5 mm in diameter, and 1.5 mm in length chopped-steel fibers delivered in a compressed (0.54 MPa) air stream for 20 minutes (approximately 100% coverage), that is until maximum Almen intensity was achieved.

Hardness and residual stress measurements. The hardness traverse was measured using Leitz microhardness tester with Knoop indenter and a load of 2 N. The longitudinal (axial) surface residual stresses were measured using an X-ray residual stress apparatus. The irradiated spot was 2.5 mm in diameter with an X-ray surface penetration depth less than 5 μm.

Fatigue testing. Specimens were fatigue tested in a 20 kip servo-hydraulic material testing system (MTS) machine with self-aligning grips using a sine wave form, load control, a zero-to-max. stress cycle (stress ratio was equal to zero), and a test frequency of 15 Hz. Two micro-measurements strain gauges (6.4 mm length and 120 Ω resistivity) were attached to both sides of each specimen using M-bond 200 adhesive (cyanocryle) to monitor bending stresses. A proper distance (one-third of the plate thickness) from the weld toe was maintained so that the monitored strain would be independent of the weld toe stress concentration and would approximate the nominal surface strain.

RESULTS AND DISCUSSION

Hardness

Knoop hardness traverse results for as-welded and post-weld treated samples are plotted in Fig. 4. The data indicate a decrease in the hardness of the laser-shocked specimens just under the surface (0.01 mm from the surface), a slight increase at the depth of 0.05 mm and a constant hardness beyond of 0.1 mm. The decrease in hardness, near the surface, could be attributed to a new phase formed due to the thermal effect of the laser beam. The hardness increase in the deeper layers of the shocked sample is assumed to be a result of the material plastic deformation and a consequent increase in the dislocation density. Shot peening gave about 20% increase in hardness at the vicinity of surface which declined to the hardness of as-welded specimens at the depth of 0.25 mm.

Fatigue

Fatigue test results. Figure 5 shows the fatigue data and their linear-regression representations for as-welded, laser-treated, and peened specimens. Since two kinds of specimens were used in this study, the fatigue test results were plotted using local stresses versus fatigue life rather than nominal stresses. The (K_{fmax}) concept [14] was used to estimate the effect of stress concentration factor on the fatigue strength. There is a little difference in a slope of the regression lines and the slope is rather small. It means that an initiation and early growth was the major portion of the fatigue life rather than propagation. They showed, however, much better performance than as-welded specimens; for fatigue life equal to 2 million cycles that difference was approximately 20%. We believe that this could be attributed to the increased hardness (Fig. 4) and induced, during the post-weld treatment, compressive residual stresses (Table 3).

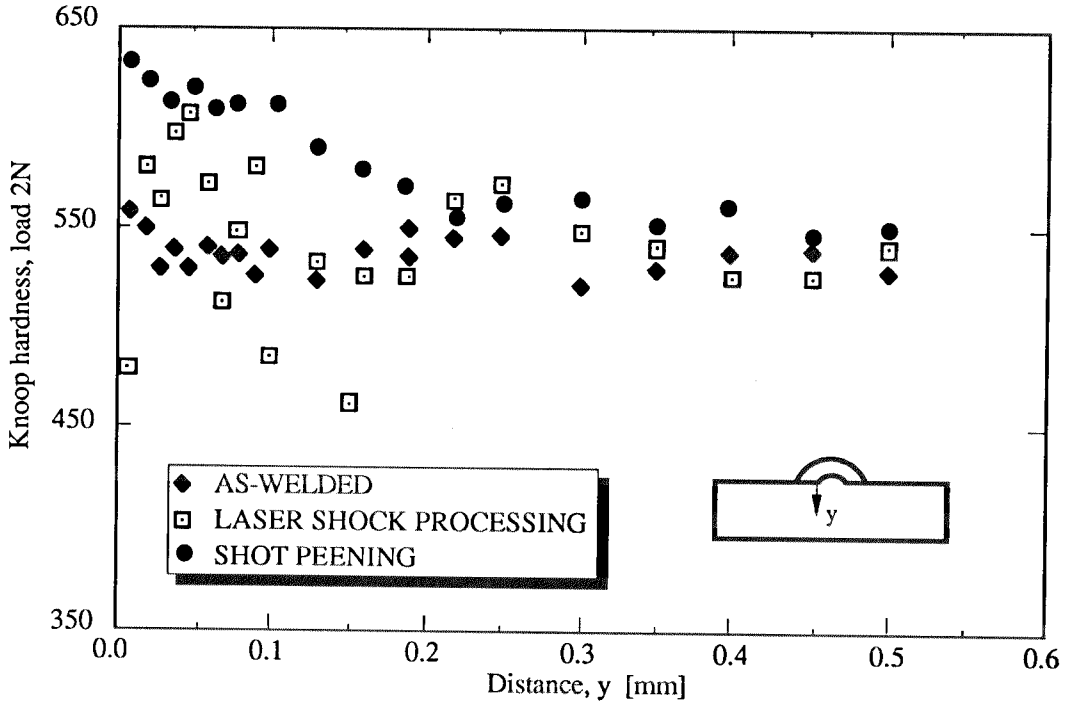

Fig. 4 Knoop hardness traverse for as-welded, laser-treated, and peened specimens measured in (y) direction from the weld toe surface.

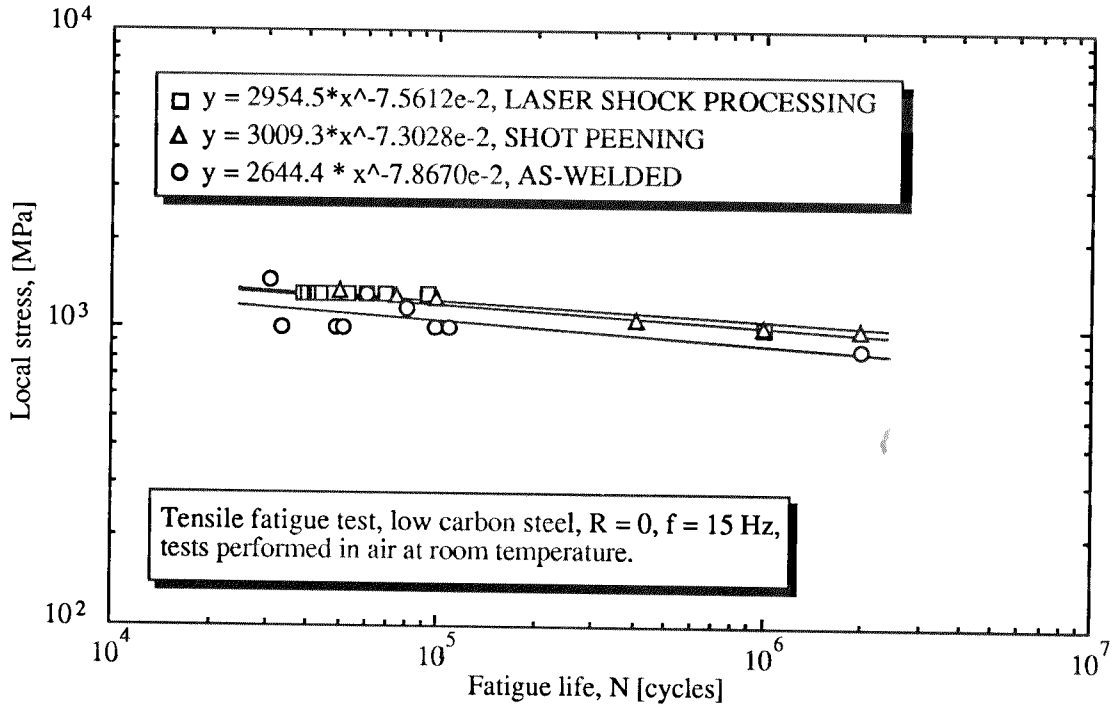

Fig. 5 Local stress at the weld toe versus fatigue life for as-welded, laser-treated, and shot-peened specimens.

Fatigue strength predictions. Yung and Lawrence [14] have developed an expression for the fatigue strength predictions of weldments by considering crack initiation and early growth:

$$S_a = \frac{(\sigma_f' - \sigma_r)\,(2N_I)^b}{K_{fmax}^{eff}\left[1 + \frac{1+R}{1-R}(2N_I)^b\right]} \tag{1}$$

where:

S_a - remote stress amplitude,

σ_f' - fatigue strength coefficient,

σ_r - residual stress at the notch root,

$2N_I$ - number of reversals,

b - fatigue exponent,

R - stress ratio, and

K_{fmax}^{eff} - effective fatigue notch factor for the worst-case notch value which can be calculated using the following expression:

$$K_{fmax}^{eff} = \left(1 - \frac{S_a^B}{S_a^A + S_a^B}\right) K_{fmax}^{A} + \frac{S_a^B}{S_a^A + S_a^B} K_{fmax}^{B} \tag{2}$$

where:

K_{fmax}^{A} - maximum fatigue notch factor for axial load,

K_{fmax}^{B} - maximum fatigue notch factor for bending load,

S_a^A - axial remote stress amplitude, and

S_a^B - bending remote stress amplitude.

Peterson's equation [14] correctly interrelates the fatigue notch and elastic stress concentration factors:

$$K_f = 1 + \frac{K_t - 1}{1 + \frac{a}{r}} \tag{3}$$

where:

K_t - elastic stress concentration factor for a given notch geometry,

r - notch-root-radius,

K_f - fatigue notch factor, and

a - Peterson's material parameter.

The (K_{fmax}) occurs at the notch radii numerically equal to Peterson's parameter (a) (r_c = a):

$$K_{fmax} = 1 + \frac{K_t - 1}{2} \tag{4}$$

Elastic stress concentration factor (K_t) was determined using finite element analysis considering both tensile and bending stresses. The notch radius was determined from measurements. It was equal to 0.1 mm. Both parameters of Eq. 1, (σ_f') and (b) , are related to tensile strength and can be estimated

from hardness measurements. McMahon [15] assumed a linear relationship between (σ_f') and hardness:

$$\sigma_f' = 3.3\ DPH + 370 \approx 0.95\ S_u + 400 \quad (MPa) \tag{5}$$

where:

DPH- diamond pyramid hardness (Vickers), and
S_u - ultimate tensile strength.

There is a general trend of (b) decreasing in absolute value with increasing hardness [15]. A relationship commonly used to relate (b) to the hardness (or ultimate strength) is:

$$b = -\frac{1}{6}\log\left(\frac{2\sigma_f'}{S_u}\right) = -\frac{1}{6}\log\left(\frac{2DPH + 1380}{DPH}\right) \tag{6}$$

Table 3 Predicted and experimental fatigue strength results at $2x10^6$ cycles.

Description	Residual stresses [MPa]	Nominal fatigue strength [MPa]	
		experimental	predicted
As-welded	-280	315	296
Laser shock processing	-416	380	346
Shot peening	-893	587	478

The fatigue strength at $2x10^6$ cycles of as-welded, laser-treated, and peened samples were calculated using Eq. 1. Results of those calculations are listed in Table 3. Despite the small number of fatigue data points, particularly for as-welded and peened specimens, the predictions are consistent with the experimental results for as-welded and laser-treated specimens (approximately 10% difference), and the predictions are less consistent (approximately 20% difference) for peened specimens. The fatigue strength predicted using Eq. 1 was systematically higher than experimental results, suggesting an under estimation of the fatigue notch factor by the $\left(K_{fmax}^{eff}\right)$ concept for very small weldments.

CONCLUSIONS

1. Laser shock processing with 10^{12} W/cm^2 power density and shot peening altered the hardness and residual stresses of welded 18 Ni (250) maraging steel to the depth of 0.05 mm and 0.25 mm respectively.

2. Laser shock processing and shot peening increased the fatigue strength at $2x10^6$ cycles by approximately 20% for the 18 Ni (250) weldments.

3. The fatigue strength predicted using crack initiation and early growth was approximately 10 -20% higher than experimental results. The difference could be attributed to an under estimation of the fatigue notch factor (K_f).

4. Laser shock processing has been found to be a prospective strain hardening technique which may replace conventional methods in the near future.

REFERENCES

[1] Ready, J. F. "Laser Processing - The First 20 Years". Proceedings of the First International Laser Processing Conference, Anahem, California, (1981).

[2] Ferris, S. D., et al. Editors, "Laser-Solid Interactions and Laser Processing - 1978". American Institute of Physics, New York, (1979).

[3] Gibbons, J. F., et al. Editors, "Laser and Electron-Beam Solid Interactions and Materials Processing". Elsevier North Holland, Inc. New York, (1981).

[4] White, C. W. and Peercy, P. S. "Laser and Electron Beam Processing of Materials". Academic Press, Inc., New York, (1980).

[5] Mukherjee, K. and Mazumdar, J. Editors, "Lasers in Metallurgy". A Publication of the Metallurgical Society of AIME, (1981).

[6] Mordike, B. L. Editors, "Laser Treatment of Materials". DGM Informationsgesellschaft - VERLAG, (1986).

[7] Mazumdar J., "The State-of-the-Art of Laser Materials Processing". Interdisciplinary Issues in Materials Processing and Manufacturing, presented at The Winter Annual Meeting of The American Society of Mechanical Engineers, Boston (1987).

[8] Fairand, B. P., et al. "Laser Shock Induced Microstructural and Mechanical Property Changes in 7075 Aluminum". Journal of Applied Physics, Vol. 43, No. 9, p. 3893, Sept. (1972).

[9] Hsu, T. R. "Applications of the Laser Beam Technique to the Improvement of the Metal Strength". Journal of Testing and Evaluation, Vol. 1, No. 6, p. 457, (1973).

[10] Ford, S. C., et al., "Investigation of Laser Processing -- Executive Summary". Application of the Laser in Metalworking, American Society for Metals, (1981).

[11] Banaś G. and Łunarski, J., Report on "Badania wpływu umocnienia na wytrzymałość złaczy spawanych ze stali N18K9M5TPr". Politechnika Rzeszowska, Poland (1983).

[12] Socie, D. F., Mitchel, M. R., and Caulfield, E. M., FCP Report No. 26, College of Engineering, University of Illinois at Urbana-Champaign (1978).

[13] Fairand, B. P. and Clauer,A. H., Opt. Commun. 18, 588 (1976).

[14] Yung, J. -Y. and Lawrence, F. V. Jr., Fatigue Fract. Engng Mater. Struct. 8, 223 (1985).

[15] McMahon, J., "Predicting Fatigue Properties Through Hardness Measurements". M. S. Thesis, University of Illinois at Urbana-Champaign (1984).